JACS
JOURNAL OF THE AMERICAN CHEMICAL SOCIETY
Article
pubs.acs.org/JACS

Deprotonation of *p*-Hydroxybenzoic Acid: Does Electrospray Ionization Sample Solution or Gas-Phase Structures?

Detlef Schröder,[†] Miloš Buděšínský,[†] and Jana Roithová*[,‡]

[†]Institute of Organic Chemistry and Biochemistry, Flemingovo nám. 2, 16610 Prague 6, Czech Republic

[‡]Department of Organic Chemistry, Faculty of Sciences, Charles University in Prague, Hlavova 8, 12843 Prague 2, Czech Republic

Supporting Information

ABSTRACT: Despite the simplicity of the molecule, the site of single deprotonation of *p*-hydroxybenzoic acid upon electrospray ionization (ESI) has recently formed a subject of debate in this journal. By means of NMR experiments in solution and gas-phase studies employing ion-mobility mass spectrometry (IM-MS), the apparent controversy is resolved. It is shown that irrespective of the solvent the carboxylate tautomer is preferred in solution, while the opposite holds true for isolated ions in the gas phase. The tautomer distribution sampled in the gas phase very much depends on the actual solvent used in ESI, the pH value, as well as the total concentration. Moreover, the occurrence of gas-phase reactions in the course of the ESI process influences the tautomer ratio. Implications for correlations between ESI mass spectra and solution-phase chemistry are discussed.

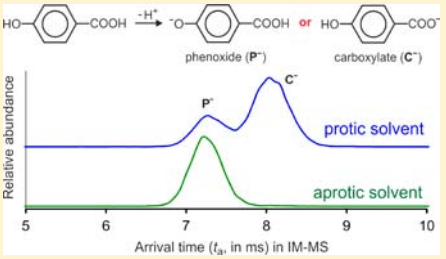

1. INTRODUCTION

Ambient ionization methods are becoming not only more and more successful in a variety of analytical applications but are often assumed to allow a sampling of solution-phase properties by mass spectrometric means.[1] In this respect, two recent communications in this journal[2−4] challenged the state of knowledge for the seemingly trivial case of the deprotonation of *p*-hydroxybenzoic acid (**1**). The specific question in this respect is whether single deprotonation of **1** leads to the carboxylate ion $\mathbf{C}^-$ or the phenoxide ion $\mathbf{P}^-$ (Scheme 1). In this context, it

Scheme 1. Single Deprotonation of 1 To Afford Either the Carboxylate $\mathbf{C}^-$ or the Phenoxide $\mathbf{P}^-$

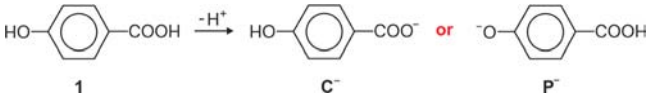

is important to note that deprotonation of **1** represents one of the cases in which the relative stabilities of the monoanionic tautomers differ between the isolated anions in the gas phase and the solvated species in the bulk.[5−7] A simple rationale for the reversal of stabilities is that in the free phenoxide the charge is largely delocalized, thereby stabilizing this tautomer compared to the carboxylate having a high charge density. In turn, the latter experiences larger solvation energy in solution, which overcompensates the stability difference of the free ions and thus renders $\mathbf{C}^-$ more stable in the liquid phase.

In the previous communications on this subject, several important observations were made. First, Tian and Kass (TK)[2a] reported a pronounced effect of the solvent used in electrospray ionization mass spectrometry (ESI-MS) on the distribution of the tautomers observed in the gas phase. According to their results, the ion formed from acetonitrile solution easily undergoes decarboxylation upon collision-induced dissociation (CID) and exchanges one proton for deuterium in the presence of trifluoroethanol, whereas the tautomer formed from methanol/water neither looses CO_2 nor undergoes H/D exchange. Upon the basis of these observations, TK assigned the ion generated from aprotic acetonitrile to the carboxylate $\mathbf{C}^-$, whereas they argued that the use of protic solvents such as methanol/water permits tautomerization to the more stable gas-phase tautomer $\mathbf{P}^-$ in the course of the ESI process. While subsequently Steill and Oomens (SO)[3] fully confirmed the decisive effect of the solvent on the tautomers observed in the gas phase, their spectroscopic investigations of the gaseous ions found characteristic ν_{COOH} and ν_{COH} modes for the ion made from acetonitrile but symmetric and asymmetric ν_{COO^-} modes for the ions generated from protic solvents. Accordingly, SO came to the opposite structural assignment, i.e., generation of $\mathbf{P}^-$ from aprotic and $\mathbf{C}^-$ from protic solvents. Moreover, TK and SO differ in the conclusions with respect to the correlation between ESI mass spectra and the situation in solution. TK argued that the carboxylate prevails in solution, whose structure is preserved when using aprotic solvents, whereas protic solvents permit protonation/deprotonation sequences to the more stable gas-phase ion $\mathbf{P}^-$. Thus, the solution structure is not maintained upon transfer to the gas phase. In contrast, SO argued that due to differential solvation effects the phenoxide tautomer already prevails in aprotic solvents, while $\mathbf{C}^-$ is preferred in protic media. In consequence, these authors concluded that ESI-MS directly reflects the solution-phase structures.

Received: June 27, 2012
Published: August 29, 2012

   dx.doi.org/10.1021/ja3060589 | J. Am. Chem. Soc. 2012, 134, 15897−15905

Such a situation is both scientifically unsatisfactory and a challenge. The key questions can be summarized as follows. Which of the tautomers is preferred in protic and aprotic solvents? How to provide an unambiguous assignment of the ion structures which is consistent with the previous experimental reports? What is the influence of the ESI process on the distribution of the tautomers sampled in the gas phase? To answer these questions, we apply a combination of NMR measurements in the condensed phase and ion-mobility mass spectrometry (IM-MS)[8] of the gaseous anions in conjunction with a simple methylation strategy for structural assignment and complementary computational studies.

2. METHODS

Nuclear magnetic resonance (NMR) spectra of the title compounds in the condensed phase were recorded with a Bruker AVANCE II 600 MHz spectrometer (^{1}H at 600.13 MHz and ^{13}C at 150.9 MHz frequency) equipped with a triple-resonance 5 mm cryoprobe. Structural assignment of the carbon signals was confirmed by 2D-H,C-HSQC and 2D-H,C-HMBC spectra.

Mass spectrometric experiments were performed with a SYNAPT G2 (Waters) ion-mobility mass spectrometer.[8a,9] In brief, the instrument has an ESI source from which the ions are transferred to the vacuum manifold using a traveling waveguide. Then, the ions of interest are mass selected using a quadrupole analyzer (Q). In the ion-mobility mode, the mass-selected ions are collected in a linear ion trap (Trap) filled with argon, from which they are admitted as a single pulse via a helium cooling cell to the ion-mobility section (IMS), in which nitrogen is present at a pressure of approximately 2 mbar. After extraction from the drift tube, the ions pass a transfer cell (Trans) and enter a reflectron time-of-flight (TOF) mass spectrometer, which continuously records mass spectra with a mass resolution ($m/\Delta m$) of ca. 25 000. In the ion-mobility experiments described below, the ions of interest were mass selected using Q at unit mass resolution, and the arrival-time distributions were recorded in time steps of about 0.07 ms, required for recording and processing TOF spectra from m/z 100 to 2000. It is important to note that the absolute values of the arrival times in the SYNAPT G2 very much depend on the adjustments of the pressures and the voltage settings. Any comparison can therefore only be made relative to each other under identical settings.[10] For a given set of gas-flow rates and voltages, however, the arrival times are quite well reproducible and do not show day-to-day variations or similar imponderable effects.

Ion formation in ESI is generally sensitive to the ionization conditions, where the voltage settings in the source region have pronounced effects;[1b] in the SYNAPT, the decisive parameter is the cone voltage (U_c), which is applied at the transfer of the ions from atmospheric pressure to the vacuum system. At larger cone voltages, the ions undergo multiple collisions with the nebulizing nitrogen gas (1 bar), which increase their internal energy and may thus induce fragmentation or even atomization;[11] in the case of anions, also electron detachment can occur which leads to an apparent loss of signal without any fragment ions appearing. Anions of interest were generated by ESI of dilute solutions of the acid **1** in various solvents and concentrations with or without additives as specified further below. Solutions were infused at flow rates of 5–20 μL min^{-1}; the desolvation temperature was 200 °C, and the ESI source was kept at 80 °C.[12]

Calculations were performed using the density functional theory method B3LYP[13−16] together with the 6-311++G(2d,p) basis set as implemented in the Gaussian 09 package.[17] All reported structures represent genuine minima or transition structures on the potential-energy surfaces as confirmed by analysis of the corresponding Hessian matrices. All minima were further reoptimized using the polarized continuum model to approximate solvation effects,[18] and frequency calculations were again performed in order to control the identity of the stationary points as well as to obtain thermochemical corrections for energies at 0 K and Gibbs energies at 298 K. All optimized structures and their energies are listed in Table S1, Supporting Information.

3. RESULTS AND DISCUSSION

From the problem outlined in the Introduction evolve three obvious tasks: (i) Determination of the deprotonation site of **1** in solution, particularly with respect to protic and aprotic solvents; (ii) assignment of the structures of the deprotonated ions in the gas phase and their fragmentations; (iii) providing a comprehensive explanation of the previous and present findings with particular attention to the question if ESI-MS probes condensed-phase or gas-phase properties.

NMR Studies of 1 and Its Anions in Different Solvents. Steill and Oomens[3] argued that the different tautomers probed evolving upon ESI-MS are due to a switch of the deprotonation site of **1** in protic and aprotic solvents. On the basis of analogies with acidity series in solution, Kass and co-workers later discarded the argument.[2b] Likewise, our theoretical studies (see below) imply predominance of the carboxylate tautomer $\mathbf{C}^-$ in both water and acetonitrile solution. Nevertheless, the analogies are indirect and the computational studies in solution could be biased by the solvation model used as well as effects of explicit solvent molecules. Therefore, one of our key aims is to achieve an unambiguous assignment of the singly deprotonated form of **1** in solution to either of the tautomers $\mathbf{C}^-$ and $\mathbf{P}^-$. Figure 1 shows the results of a titration of **1** with NaOD in D_2O as followed by the shifts of the aromatic protons in ^{1}H NMR (for corresponding ^{13}C data see the Supporting Information).

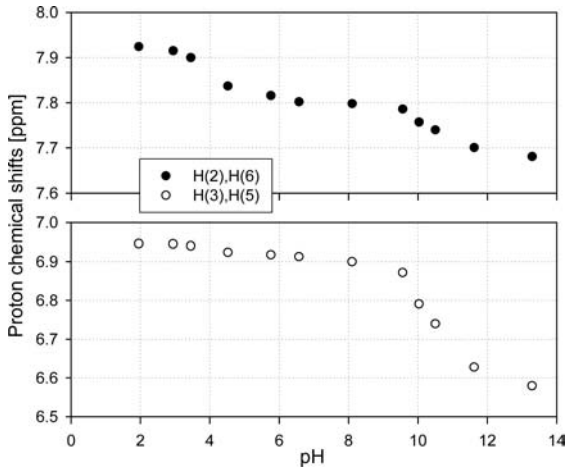

Figure 1. ^{1}H NMR chemical shifts of the aromatic protons for a solution of **1** in D_2O at different pH values; adjustment of the pH was achieved by addition of NaOD (● = C(2),C(6) protons; ○ = C(3),C(5) protons).

The chemical shift of the H(2),H(6) protons with δ = 7.92 ppm at pH = 2 shows two steps of deprotonation with inflection points at ca. pH 4.5 and 10.5, respectively, which agree favorably with the more precise first and second pK_a values of **1** available in the literature.[19] Thus, single and double deprotonation is obvious, but the central question is the assignment to an actual structure, i.e., $\mathbf{C}^-$ versus $\mathbf{P}^-$. Specifically, we should not use any assumptions and instead search for a first-principle proof of the deprotonation site. To this end, we simply considered the monomethylated compounds HO–C_6H_4–$COOCH_3$ (**2**) and H_3CO–C_6H_4–COOH (**3**), respectively, in which one of the acidic protons is selectively removed

dx.doi.org/10.1021/ja3060589 | J. Am. Chem. Soc. 2012, 134, 15897−15905

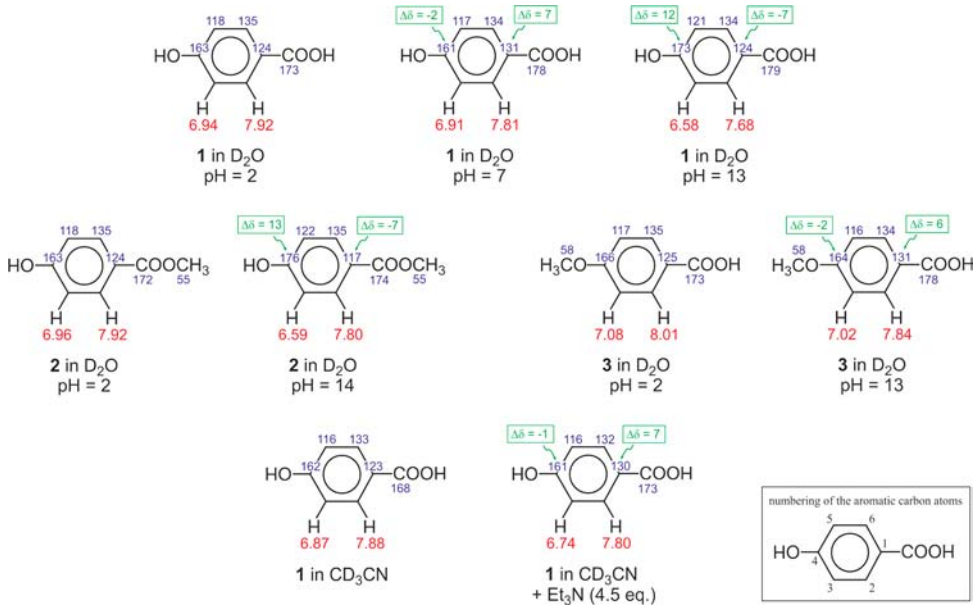

Figure 2. Chemical shifts (^{1}H in red and ^{13}C in blue; the latter rounded to full ppm) of the atoms of the aromatic rings in compounds **1**–**3** at different pH values and different solvents. In D_2O solutions, NaOD was used as a base to adjust the pH, whereas the alkali carboxylates precipitate in CD_3CN and instead Et_3N was used as a base. Green values (in boxes) indicate the differential chemical shifts of the quarternary carbon atoms C(1) and C(4). Numbering of the carbon atoms is defined in the right bottom.

by derivatization. Consequently, deprotonation of **2** only can afford the corresponding phenoxide labeled as $\mathbf{P}_{\mathbf{Me}}^-$, and **3** can only yield the carboxylate $\mathbf{C}_{\mathbf{Me}}^-$. Results of the corresponding series of ^{1}H and ^{13}C NMR experiments in different solvents and at variable pH are summarized in Figure 2.

Analysis of the data is made somewhat more complicated by the significantly different chemical shifts in D_2O and CD_3CN. For interpretation, let us therefore focus on the quarternary aromatic carbon atoms C(1) and C(4) which are least affected by solvation and their chemical shifts are indeed almost identical in D_2O and CD_3CN, respectively. As highlighted by the chemical shift differences ($\Delta\delta$) given in Figure 2, the first deprotonation of **1** in D_2O shifts C(1) by $\Delta\delta$ = 7 ppm and C(4) by $\Delta\delta$ = −2 ppm. Within experimental error, identical shift differences are observed for deprotonation of **3** to afford the carboxylate $\mathbf{C}_{\mathbf{Me}}^-$, whereas the phenoxide $\mathbf{P}_{\mathbf{Me}}^-$ formed from **2** shows opposite shifts of $\Delta\delta$ = −7 ppm for C(1) and $\Delta\delta$ = 13 ppm for C(4). The differential chemical shifts of the quarternary carbons are almost perfectly additive in that for the dianion formed from **1** at pH 13 the positive and negative differences cancel for C(1) and add up for C(4). From these observations we can safely conclude that deprotonation of **1** in protic solvents leads to the carboxylate tautomer, which was obvious from the beginning but still needed to be established firmly. With this information in hand, the differential shifts of $\Delta\delta$ = 7 ppm for C(1) and $\Delta\delta$ = −1 ppm for C(4) observed upon addition of triethylamine as a base to a solution of **1** in CD_3CN clearly demonstrate the predominance of tautomer $\mathbf{C}^-$ also in aprotic solvents, as suggested by TK.[2] The speculation of SO that tautomer $\mathbf{P}^-$ might indeed be preferred in aprotic solvents therefore is to be denied.[3]

IM-MS Measurements of Deprotonated *p*-Hydroxybenzoic Acid. The first task was to probe whether or not tautomers $\mathbf{C}^-$ and $\mathbf{P}^-$ have different arrival times (t_a) in IM-MS and, if so, to unambiguously assign the possibly separated features in IM-MS to a certain structure. Already a first test with a ca. 10^{-3} M solution of the free acid **1** in water demonstrated that IM-MS is well capable to separate both isomers without the need of variation of the buffer gas in the ion-mobility unit or any other more sophisticated efforts (Figure 3).[20] Hence,

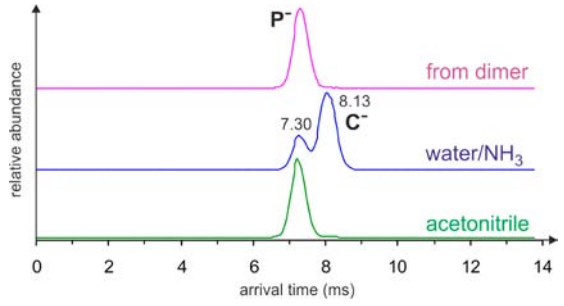

Figure 3. Arrival-time distributions of the mass-selected anion with m/z 137 generated upon ESI of a ca. 10^{-3} M solution of **1** in acetonitrile (green) and water with a trace of NH_3 (blue). Top trace (pink) shows the same ion generated upon dissociation of the mass-selected proton-bound dimer (m/z 275) prior to injection into the ion-mobility unit; for all solvents used, only the early component was obtained from the proton-bound dimer.

under standard conditions of the SYNAPT instrument (ca. 2 mbar N_2, arrival times adjusted to several milliseconds), tautomers $\mathbf{C}^-$ and $\mathbf{P}^-$ (both m/z 137) can be distinguished, thereby providing the basis for a comprehensive investigation of the title problem. Specifically, two components are observed at arrival times of $t_{a,early}$ = (7.30 ± 0.04) ms and $t_{a,late}$ = (8.13 ± 0.04) ms (Δt_a = 0.83 ± 0.06 ms); for the limited significance of the absolute values of t_a, see the discussion in the experimental details.

The results shown in Figure 3 further fully support the previous observations that the relative populations of the two tautomers sampled in the gas phase are crucially influenced by the solvent used in ESI-MS. Further, Figure 3 includes the arrival-time distribution for the ion with m/z 137 obtained

dx.doi.org/10.1021/ja3060589 | J. Am. Chem. Soc. 2012, 134, 15897−15905

upon mass selection of the proton-bound dimer $[\mathbf{1}_2\text{-H}]^-$ (m/z 275) followed by its dissociation upon injection into the ion-mobility section (pink trace on top). Interestingly, this experiment exclusively leads to the early component, which can be explained by reference to Cooks' kinetic method[21] as detailed further below.

For the structural assignment of the early and late components in the IM-MS experiments, we applied the same monomethylation strategy as in the NMR studies. Thus, deprotonation of the methylester **2** leads to an ion with m/z 151 having an arrival time of $t_a([\mathbf{2}\text{-H}]^-)$ = 8.47 ms, whereas under identical conditions the m/z 151 anion formed from **3** shows $t_a([\mathbf{3}\text{-H}]^-)$ = 9.21 ms; thus, Δt_a = 0.74 ms. Because deprotonation of **2** can only yield a phenoxide and that of *p*-methoxybenzoic acid (**3**) only a carboxylate, in the case of the two $[\mathbf{1}\text{-H}]^-$ ions the early component is accordingly assigned to the phenoxide ion $\mathbf{P}^-$ and the late component to the carboxylate tautomer $\mathbf{C}^-$.

In this context, a more general comment on IM-MS appears indicated. Nowadays, many scientists promote IM-MS as a size-selective analysis of gaseous ions which can sensitively distinguish between isomers of different shapes (e.g., conformers) relying on the key assumption that ion mobilities are primarily determined by the respective hard-sphere collision cross sections.[22] The pairs $\mathbf{P}^-/\mathbf{C}^-$ and $\mathbf{P_{Me}}^-/\mathbf{C_{Me}}^-$ clearly demonstrate that size is not the only decisive parameter in IM-MS, because the size of the anions is not affected by the site of the molecule to which the proton or a methyl group is connected. As demonstrated in seminal papers of Bowers and co-workers about ion chromatography,[23] another key factor determining ion mobility is the strength of interaction of the ionic species with the neutral bath gas. Instead, it appears that the nitrogen gas acting as moderator in IM-MS is actively engaged in interactions with the isomeric anions. In this respect, consideration of the computed charge distributions can indeed account for the difference in that the negative charge is largely delocalized in the phenoxide $\mathbf{P}^-$, whereas it is mostly localized at the carboxy group in the case of the carboxylate $\mathbf{C}^-$ (Scheme 2). Hence, ion/(induced)dipole interactions will be much more pronounced for tautomer $\mathbf{C}^-$, thereby accounting for the enlarged arrival time relative to $\mathbf{P}^-$.

Scheme 2. Computed Charge Distributions and Dipole Moments[24] of the Phenoxide Ion $\mathbf{P}^-$ (left) and Carboxylate $\mathbf{C}^-$ (right)

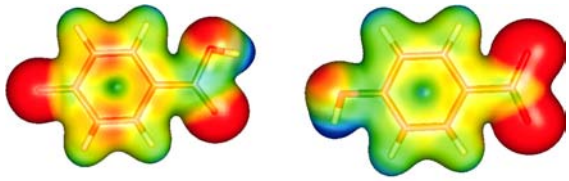

After this initial assay, let us address the effects of different solvents as well as additives on the ratio of the tautomers in the gas phase as sampled by IM-MS. The data in Table 1 demonstrate that the solvent composition has a decisive effect on the relative fractions of tautomers $\mathbf{P}^-$ and $\mathbf{C}^-$. In pure acetonitrile (entry 1), the phenoxide ion $\mathbf{P}^-$ is observed almost exclusively, while the fraction of the carboxylate ion $\mathbf{C}^-$ increases upon addition of triethylamine as a base (entries 1 and 2). The ratios of the tautomers observed from methanol/water strongly depend on the absolute concentration of the analyte with tautomer $\mathbf{C}^-$ being increasingly favored at larger dilutions (entries 3–5). Pure water as a solvent even further increases the fraction of ion $\mathbf{C}^-$ (entry 6) as does addition of ammonia as a base (entry 8). In order to test the possibility of gas-phase reactions occurring in the source region, we also admitted an additional flow of pure water to the source region via the lock-spray device of the instrument. Direct mixing of the droplets from both sprayers is prevented by a mechanical deflector, such that the additional water flow (10 times larger than that of the analyte solution) primarily leads to an increased vapor pressure of water in the source region. Compared to the respective entries 6 and 8 serving as references, the experiments with additional water being present lead to a significant increase of the population of $\mathbf{P}^-$ (entries 7 and 9), lending strong support to the argument of TK that protic solvents can mediate proton transfer in the gas phase going from the less stable gas-phase ion $\mathbf{C}^-$ to the more stable tautomer $\mathbf{P}^-$.[2] In general, however, the trends regarding the populations of tautomers $\mathbf{P}^-$ and $\mathbf{C}^-$ observed in the gas phase depending on the ESI solvents are in good agreement with the assignments made by SO.[3]

Table 1. Fractions of Tautomers $\mathbf{P}^-$ and $\mathbf{C}^-$ As Derived from the Arrival-Time Distributions of the Mass-Selected Anion with m/z 137 Generated upon ESI with Variable Solvents and Analyte Concentrations[a]

entry	solvent	$c(\mathbf{1})/\mathrm{M}^b$	$\mathbf{P}^-$	$\mathbf{C}^-$
1	CH_3CN	10^{-3}	100	2
2	CH_3CN + Et_3N^c	10^{-3}	100	15
3	CH_3OH/H_2O (1:1)	10^{-3}	100	10
4	CH_3OH/H_2O (1:1)	10^{-5}	100	45
5	CH_3OH/H_2O (1:1)	10^{-7}	100	90
6	H_2O	10^{-5}	90	100
7	H_2O/H_2O (lock)[d]	10^{-5}	100	35
8	H_2O + NH_3^c	10^{-5}	40	100
9	H_2O + NH_3^c/H_2O (lock)[d]	10^{-5}	85	100

[a]Ratios reported in the table were all obtained under soft ionization conditions (U_c = 10 V) at a flow rate of 5 μL min^{-1} and default temperatures of 200 (desolvation) and 80 °C (source); for the influence of the ionization conditions, see text. [b]Approximate concentration of **1** in the sample solution; for more accurate concentration dependence, see below. [c]Approximate concentration 10^{-2} M. [d]Notation "H_2O (lock)" stands for an additional feed of pure water (50 μL min^{-1}) to the ESI source via the lock-spray device of the SYNAPT G2; the lock spray capillary was grounded in these experiments.

In addition, the ionization conditions in the ESI source have some effects on the ratio of the tautomers, which are more subtle however and hence only reported briefly. Upon harshening of the ionization conditions by raising the cone voltage U_c, the fraction of $\mathbf{C}^-$ slightly increases in methanol/water while it decreases for acetonitrile as a solvent. Lowering the temperatures in the ESI source as well as higher flow rates of the sample lead to gradual increases of fraction $\mathbf{C}^-$. These observations can be rationalized by assuming that the tautomerization of $\mathbf{C}^-$ into the more stable gas-phase isomer $\mathbf{P}^-$ is associated with a barrier when mediated by protic solvent molecules in the gas phase of the source region. In turn, the decrease of fraction of $\mathbf{C}^-$ at larger cone voltages in the case of acetonitrile can be attributed to dissociation of the proton-bound dimer, which only affords tautomer $\mathbf{P}^-$ (see upper trace in Figure 3).

dx.doi.org/10.1021/ja3060589 | J. Am. Chem. Soc. 2012, 134, 15897–15905

One particular aspect of Table 1 is the pronounced effect of the analyte concentration on the ratio of fractions of $\mathbf{P}^-$ and $\mathbf{C}^-$. Figure 4 shows the results for a concentration series in

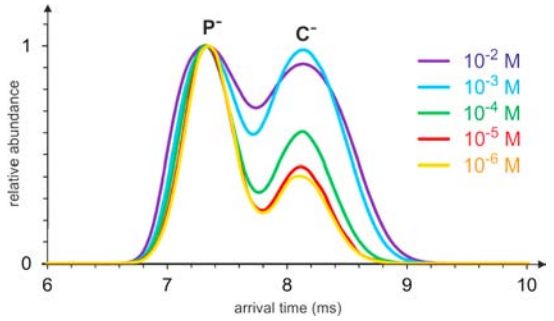

Figure 4. Arrival-time distributions of the mass-selected anion with m/z 137 generated upon ESI of different concentrations of **1** dissolved in methanol/water (1:1) containing 6×10^{-4} M NH_3.

methanol/water with a constant amount of ammonia ($c(NH_3) = 6 \times 10^{-4}$ M).[25] In the most dilute solutions, the peak with the early arrival time, i.e., the phenoxide, prevails largely, whereas the fraction of the late peak, i.e., the carboxylate, increases at higher concentrations, and a ca. 1:1 ratio is reached at $c(\mathbf{1}) = 10^{-3}$ M. This trend can be attributed to increasingly larger amounts of the carboxylate $\mathbf{C}^-$ present in solution, while the gas-phase isomerization to form $\mathbf{P}^-$ remains constant. For the 10^{-2} M solution, the fraction of $\mathbf{C}^-$ slightly decreases again, which can attributed to the concentrations used in this particular concentration series, because for $c(\mathbf{1}) = 10^{-2}$ M the concentration of the acid significantly exceeds that of the base ($c(NH_3) = 6 \times 10^{-4}$ M), such that the free acid and the proton-bound dimers contribute to ion formation.[26]

Having achieved deeper insight into formation of tautomers $\mathbf{P}^-$ and $\mathbf{C}^-$ upon ESI, let us now return to the additional arguments raised by TK and SO, respectively.[2,3] The former authors used the observed decarboxylation as a key argument for structural assignment of the two tautomers in assuming that loss of CO_2 occurs from the free carboxylate. The configuration of the SYNAPT G2 instrument permits one to perform a collision-induced dissociation (CID) experiment after separation of the components via their differential mobilities. Figure 5 shows the results of such CID experiments for the two tautomers, which apparently both undergo loss of CO_2, while under identical conditions decarboxylation is more facile for $\mathbf{P}^-$. Thus, TK as well as SO are correct in their arguments in that decarboxylation is more facile for the ion made from acetonitrile solution and that both ions undergo identical fragmentations.[2,3]

From the qualitative consideration in Figure 5, we can go one step further by analyzing the energy dependence of decarboxylation upon CID,[27] which shows that loss of CO_2 from $\mathbf{C}^-$ has a higher apparent threshold than decarboxylation of $\mathbf{P}^-$ (Figure 6). Depending on the activation energy in CID, it

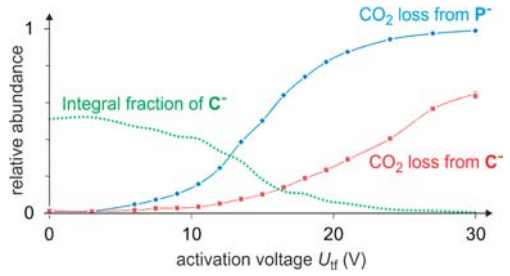

Figure 6. Fragment appearance curves (loss of CO_2) upon CID of the arrival-time and mass-selected tautomers $\mathbf{P}^-$ (blue) and $\mathbf{C}^-$ (red), both m/z 137, generated upon ESI of a 1.2×10^{-5} M solution of **1** in methanol/water (1:1) containing 6×10^{-4} M NH_3 as a function of the collision voltage (U_{tf} in V) applied. Green line shows the integrated fraction of the ion with the late arrival time (i.e., tautomer $\mathbf{C}^-$ and its fragments) during these experiments.[28].

is thus possible to realize a situation with almost exclusive fragmentation of $\mathbf{P}^-$, as reported by TK,[2] or to obtain similar CID patterns for both tautomers, as argued SO.[3] Interestingly, the total fraction of tautomer $\mathbf{C}^-$ shows a drastic decrease at elevated collision energies (green line in Figure 6). Mere fragmentation cannot account for this effect because the decarboxylation product is included in the integrated abundance of the late component.[28] Likewise, a collision-induced tautomerization would not explain the experimental results because the CID occurs after the mobility separation and any $\mathbf{P}^-$ formed eventually would thus still appear at the arrival time of $\mathbf{C}^-$. Instead, we propose the occurrence of electron detachment from the $HO{-}C_6H_4^-$ anion formed upon decarboxylation of $\mathbf{C}^-$ (see below).

The second argument on which TK based the structural assignment of the tautomers was the observation of a single H/D exchange with the ion generated from acetonitrile solution, whereas the tautomer generated from protic solvents did not undergo exchange.[2] In order to test this aspect using IM-MS, we used a solution of **1** in pure D_2O, mass selected the monodeuterated ion with m/z 138, and followed its exchange in the ion-mobility section by monitoring the unlabeled ion with m/z 137.[29] The results shown in Figure 7 clearly demonstrate that the earlier component and hence the phenoxide ion preferentially undergo H/D exchange, which is fully consistent with the experimental finding of TK that H/D

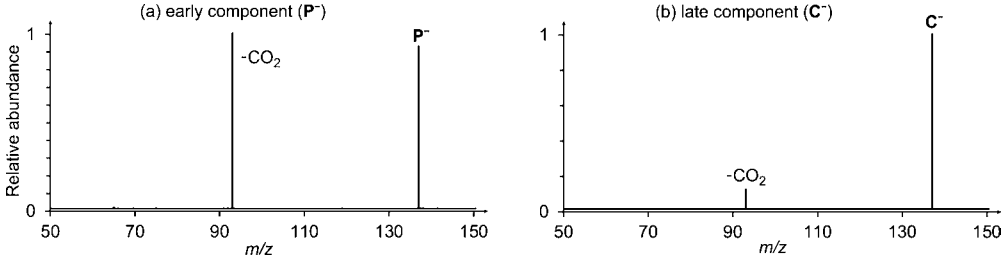

Figure 5. Transfer CID spectra of the arrival-time and mass-selected anions with m/z 137 generated upon ESI of a 1.2×10^{-5} M solution of **1** in methanol/water (1:1) containing 6×10^{-4} M NH_3: (a) early component tautomers $\mathbf{P}^-$ and (b) late component tautomer $\mathbf{C}^-$. These spectra were taken at U_{tf} = 15 V (see Figure 6).

dx.doi.org/10.1021/ja3060589 | J. Am. Chem. Soc. 2012, 134, 15897−15905

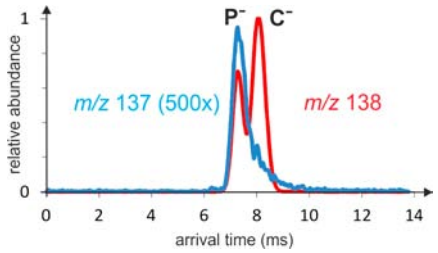

Figure 7. Arrival-time distributions of the mass-selected anion with m/z 138 generated upon ESI of ca. 10^{-5} M **1** in D_2O (red) and of the ca. two orders less abundant product of H/D exchange with protons present in the background m/z 137 (blue). Obviously, the earlier component, tautomer $\mathbf{P}^-$, exchanges much more efficiently than the late component, tautomer $\mathbf{C}^-$. The tailing observed is in fact typical for reactive collisions in IM-MS and can be ascribed to formation of transient adducts during passage through the ion-mobility unit which have a larger m/z ratio and hence larger t_a.[9b]

exchange occurs for the ion made from acetonitrile solution but disagrees with regard to the assignment in that $\mathbf{P}^-$ rather than $\mathbf{C}^-$ is prone to H/D exchange.[2]

Relevant Theoretical Findings. As a complement to the above-mentioned experimental work, we performed computational studies of the title system using density functional theory. For the gaseous ions, the calculations reproduce the expected larger stability of the phenoxide tautomer $\mathbf{P}^-$. Upon including solvation effects, the relative stabilities invert, however, both in water as well as in acetonitrile (Table 2).

Table 2. Relative B3LYP/6-311++G(2d,p) Energies (in kJ mol^{-1}) of the Deprotonated Forms $\mathbf{C}^-$ and $\mathbf{P}^-$ in the Gas Phase and Solution, Respectively, As Well As the Energetics of Decarboxylation in the Gas Phase

	gas phase		solution[a]		
	none		H_2O	H_2O[b]	CH_3CN
solvent	$\Delta\Delta H_0$	$\Delta\Delta G_{298}$	$\Delta\Delta G_{298}$	$\Delta\Delta G_{298}$	$\Delta\Delta G_{298}$
HO–C_6H_4–COO^- ($\mathbf{C}^-$)	34	33	−11	−10	−9
HO–$C_6H_4^-$ + CO_2	258	215			
HO–$C_6H_4^\bullet$ + e^- + CO_2[c]	334	290			
$^-$O–C_6H_4–COOH ($\mathbf{P}^-$)	0	0	0	0	0
TS[d]	176	175			
$C_6H_5O^-$ + CO_2	35	−6			
$C_6H_5O^\bullet$ + e^- + CO_2[e]	249	206			

[a]Solvation in the given media is approximated by the polarized continuum model (PCM). [b]Energetics with one explicit water molecule included in geometry optimization. [c]Electron detachment from the hydroxylphenyl anion formed via decarboxylation of $\mathbf{C}^-$. [d]Transition structure (TS) for the decarboxylation of the COOH group in $\mathbf{P}^-$, see Scheme 3. [e]Electron detachment from the phenoxide ion formed via decarboxylation of $\mathbf{P}^-$.

The theoretical results are thus perfectly consistent with the literature data and the experimental findings in this work both in the gas phase and in solution. Further, the calculations explain the depletion of the fraction of $\mathbf{C}^-$ relative to $\mathbf{P}^-$ in the collision experiments described in Figure 6. Thus, the electron affinity of HO–$C_6H_4^\bullet$ is computed as only 1.13 eV, compared to 2.21 eV for the phenoxy radical; for comparison, the experimental value for the electron affinity of the phenoxy radical is 2.25 eV.[30] Hence, electron detachment from HO–$C_6H_4^-$ is likely to occur at elevated collision energies; because free electrons escape from detection in the experimental setup, the monitored integrated fraction of $\mathbf{C}^-$ vanishes at higher collision energies.

Further, the calculations provide additional insight concerning the incorrect assignment of the decarboxylation as a characteristic fragmentation of the carboxylate isomer.[2] According to the DFT results, loss of CO_2 from $\mathbf{C}^-$ is a continuously endothermic process with an overall energy demand of 224 kJ mol^{-1} in the gas phase to afford the *p*-hydroxyphenyl anion HO–$C_6H_4^-$. However, also the intact carboxylic acid group in tautomeric $\mathbf{P}^-$ can undergo decarboxylation via a four-membered transition structure (Scheme 3) which directly affords the parent phenoxide

Scheme 3. Transition Structure for Direct Decarboxylation of the COOH Group in $\mathbf{P}^-$ To Afford $C_6H_5O^-$ + CO_2[a]

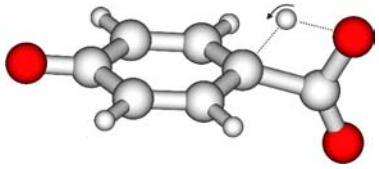

[a]Note the C_s symmetry with a perpendicular arrangement of the π systems of the benzene ring and carboxy substituent, respectively.

$C_6H_5O^-$. The corresponding energy barrier (E_{rel} = 176 kJ mol^{-1}) lies well below the exit channel to HO–$C_6H_4^-$ + CO_2, and the resulting phenoxide anion is largely energetically preferred over the *C*-deprotonated anion HO–$C_6H_4^-$ (ΔE = 223 kJ mol^{-1}). In this specific case, the occurrence of preferred decarboxylation from the gaseous ions is thus not an indication of the carboxylate structure but results from the different thermochemical demands of the final fragments.

Further, the structures of the proton-bound dimers were addressed computationally. The most stable of the gaseous dimers arises from a hydrogen bridge between a phenoxide ion $\mathbf{P}^-$ and the phenolic hydroxo group of free **1**, which is hence denoted as $[\mathbf{PHP}]^-$ in Scheme 4. The mixed dimer $[\mathbf{PHC}]^-$ is 21 kJ mol^{-1} higher in energy, which means that the energy difference between the free anions $\mathbf{P}^-$ and $\mathbf{C}^-$ (34 kJ mol^{-1}) is reduced by hydrogen bonding, but the stability order is still far from being reverse as is the case in solution. The corresponding carboxylate dimer $[\mathbf{CHC}]^-$ is accordingly still higher in energy (Scheme 4). Similar to the monomers, solvation by either methanol or acetonitrile largely stabilizes the carboxylate anions. Hence, the most stable proton-bound dimer in solution has a proton bridge between two carboxylate groups ($[\mathbf{CHC}]^-$). However, the dimer formed by bridging phenoxide and carboxylate $[\mathbf{PHC}]^-$ lies only 2 kJ mol^{-1} higher in energy in water and only 1 kJ mol^{-1} higher in energy in acetonitrile. Compared to $[\mathbf{CHC}]^-$, the $[\mathbf{PHP}]^-$ isomer is 8 kJ mol^{-1} higher in energy in water and 6 kJ mol^{-1} higher in energy in acetonitrile. Given the small energy differences, a mixture of all isomers is in fact most likely to be sampled upon electrospray ionization.

If we consider the fragmentation of the proton-bound dimers when transferred to the gas phase in the framework of Cooks' kinetic method,[21] the energies required ($\Delta G_{298,gp}$) for formation of $\mathbf{P}^-$ from $[\mathbf{PHP}]^-$ and $[\mathbf{PHC}]^-$ are 117 and 95 kJ mol^{-1}, respectively, and those for formation of $\mathbf{C}^-$ from $[\mathbf{PHC}]^-$ and $[\mathbf{CHC}]^-$ are 129 and 102 kJ mol^{-1} (Table 3). Clearly, formation of the phenoxide anion is largely energeti-

dx.doi.org/10.1021/ja3060589 | J. Am. Chem. Soc. 2012, 134, 15897−15905

Scheme 4. Computed Structures and Relative Energies (in kJ mol^{-1}) of the Possible Proton-Bound Dimers of the Tautomeric anions P$^-$ and C$^-$, Respectively, With the Free Acid 1

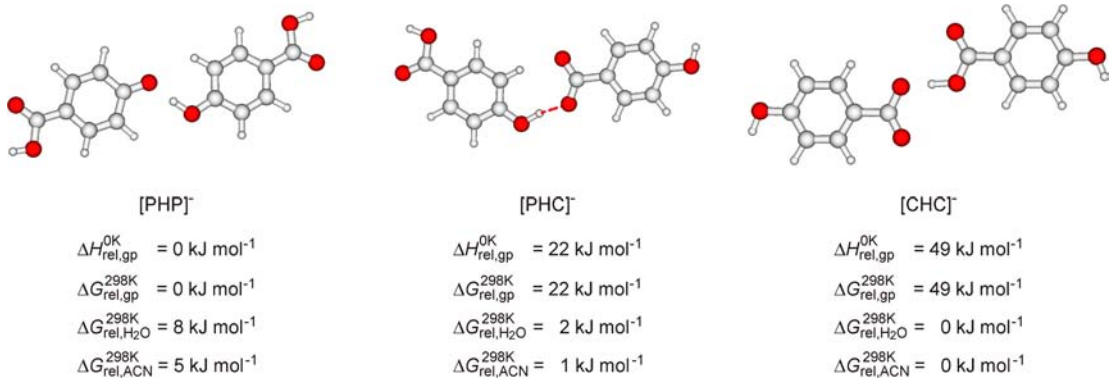

Table 3. Relative B3LYP/6-311++G(2d,p) Energies (in kJ mol^{-1}) for Dissociation of the Proton-Bound Dimers [PHP]$^-$, [PHC]$^-$, and [CHC]$^-$ in the Gas Phase and Solution, Respectively

	$\Delta\Delta H_{0,gp}$		$\Delta\Delta G_{298,gp}$		$\Delta\Delta G_{298,sol}$		$\Delta\Delta G_{298,sol}$	
solvent	none		none		H_2O		CH_3CN	
ionic fragment	P$^-$	C$^-$	P$^-$	C$^-$	P$^-$	C$^-$	P$^-$	C$^-$
[PHP]$^-$	117	*a*	75	*a*	9	*a*	10	*a*
[PHC]$^-$	95	129	53	86	14	3	14	5
[CHC]$^-$	*a*	102	*a*	59	*a*	5	*a*	6

[a]Not defined.

cally preferred, and fragmentation of [PHC]$^-$ will hence almost exclusively lead to anion P$^-$. The final ratio between tautomers P$^-$ and C$^-$ formed by fragmentation of the proton-bound dimers during electrospray ionization will thus be influenced by the equilibrium of the dimers in solution and their dissociation in the gas phase. With respect to the role of the solvent, the stabilities of the proton-bound dimers do not differ largely between water and acetonitrile, although they are slightly larger for the former, as expected. Further, the association constants derived from the computed $\Delta G_{298,sol}$ values are about K_a = 1, such that the concentrations of proton-bound dimers in the submolar samples used in the experiments are expected to be low.

Implications for Correlations between ESI-MS Measurements and Solution-Phase Properties. Finally, let us return to the debate in the literature whether or not ESI-MS samples solution-phase structures.[2,3] From the results reported above, the first direct answer is "No" in that tautomer C$^-$ prevails in solution irrespective of the solvent, whereas the ESI-MS measurements give either P$^-$ or C$^-$. Nevertheless, the obvious dependence of the outcome concerning the gaseous ions from the solvent used in electrospray suggests that there exists some relation with the situation in solution for which the answer is thus "Yes, in part". In this respect, let us consider the situation in acetonitrile in more detail. Obviously, the best solvation partner for a polar protic compound like **1** in an aprotic solvent is the compound itself,[31,32] and this effect is even expected to be more pronounced for ionic species. Moreover, the sample solutions experience an increase of concentration of the analyte in the electrospray process when the solvent evaporates from the droplets, making formation of dimers even more likely.[1,33] As outlined above, from the proton-bound dimer formation of gaseous P$^-$ is highly preferred, thereby explaining the prevalence of this tautomer from acetonitrile solution (Figure 3). In water, we might instead expect less dimers and a higher degree of heterolysis, hence increasing the population of tautomer C$^-$. The latter is even more preferred upon addition of base as demonstrated by the IM-MS experiments (Table 1). Additional complications evolve from the other relevant effects uncovered by the present measurements, such as the pH of the solution, the total concentration, as well as the obviously interfering tautomerization in a gas-phase process during the spray event. Further noteworthy in the present context is the proposal of Colussi and co-workers that ESI is in fact a surface-sensitive method in that not the bulk of the droplets but only the species present at the droplet surface are sampled in the evolving ions.[34] Hence, one may argue that the tautomers experience different degrees of enrichment/depletion on the droplet surfaces relative to the composition of the bulk. In the specific case of deprotonated *p*-hydroxybenzoic acid, involvement of such surface phenomena is unlikely to explain the changes in the populations of the two tautomers, however, because in any case the charged unit is expected to be embedded into the solvent rather than sticking out of the droplet surface.[35,36] In summary, we are far from understanding all details of the ESI process, but for the title compound the experimental and theoretical findings clearly establish the most favored deprotonation sites in the gas phase as well as solution, and the effects of varied parameters in solution on the composition of the gaseous ions demonstrate the principal existence of correlations between gas-phase measurements and solution chemistry.

4. CONCLUSIONS

Ion-mobility mass spectrometry (IM-MS) not only is a complementary tool in the analysis of biomolecules but is also very useful for structural studies of small molecules. Compared to other mass spectrometric techniques, such as CID, H/D exchange, or ion spectroscopy,[2,3,37] a major advantage of IM-MS is the direct quantitative sampling of the isomeric ions, once separation via differential mobilities can be achieved, whereas deconvolution of composite features in the more conventional mass spectrometric techniques is much more cumbersome. Thus, by means of IM-MS, in the present work we resolve a previous controversy about the assignment of the tautomeric gaseous anions formed upon single deprotonation of *p*-hydroxybenzoic acid. Complementary NMR experiments in solution demonstrate that in protic as well as aprotic solvents the carboxylate tautomer is favored, whereas experi-

dx.doi.org/10.1021/ja3060589 | J. Am. Chem. Soc. 2012, 134, 15897−15905

ment and theory show that in the gas phase the phenoxide form is preferred energetically. To some extent, both tautomers can equilibrate in the course of the ESI process and the population of the tautomers is affected by both the concentration of the analyte in solution and the solution pH, leading to a rather complex picture for the spray process. Notwithstanding, rather clear conclusions can be drawn with respect to the title question in that ESI-MS does not sample the solution structures but to a considerable extent does reflect the situation in solution, though not in a simple 1:1 fashion.

■ ASSOCIATED CONTENT

Supporting Information

Complete ^{1}H and ^{13}C NMR data for **1** and its deprotonated forms in various solvents as well as total energies and Cartesian coordinates of all theoretically studied species. This material is available free of charge via the Internet at http://pubs.acs.org.

■ AUTHOR INFORMATION

Corresponding Author

E-mail: roithova@natur.cuni.cz

Notes

The authors declare no competing financial interest.

■ ACKNOWLEDGMENTS

This work was supported by the Czech Academy of Sciences (RVO 61388963), the European Research Council (AdG HORIZOMS), and the Ministry of Education of the Czech Republic (MSM0021620857).

■ REFERENCES

(1) (a) Di Marco, V. B.; Bombi, G. G. *Mass Spectrom. Rev.* **2006**, *25*, 347−379. (b) Schröder, D. *Phys. Chem. Chem. Phys.* **2012**, *14*, 6382−6390.

(2) (a) Tian, Z.; Kass, S. R. *J. Am. Chem. Soc.* **2008**, *130*, 10842−10843. See also: (b) Schmidt, J.; Meyer, M. M.; Spector, I.; Kass, S. R. *J. Phys. Chem. A* **2011**, *115*, 7625−7632.

(3) Steill, J. D.; Oomens, J. *J. Am. Chem. Soc.* **2009**, *131*, 13570−13571.

(4) For related observations of these authors in different compounds, see also: (a) Tian, Z.; Kass, S. R. *Angew. Chem., Int. Ed.* **2009**, *48*, 1321−1323. (b) Yao, H. H.; Steill, J. D.; Oomens, J.; Jockusch, R. A. *J. Phys. Chem. A* **2011**, *115*, 9739−9749. (c) Almasian, M.; Grzetic, J.; van Maurik, J.; Steill, J. D.; Berden, G.; Ingemann, S.; Buma, W. B.; Oomens, J. *J. Phys. Chem. Lett.* **2012**, *3*, 2259−2263.

(5) McMahon, T. B.; Kebarle, P. *J. Am. Chem. Soc.* **1977**, *99*, 2222−2230.

(6) Tian, Z. X.; Wang, X. B.; Wang, L. S.; Kass, S. R. *J. Am. Chem. Soc.* **2009**, *131*, 1174−1181.

(7) For a related effect in Cs^{+} adducts of **1**, see also: Mayeux, C.; Massi, L.; Gal, J.-F.; Maria, P.-C.; Tammiku-Taul, J.; Lohu, E.-L.; Burk, P. *Collect. Czech. Chem. Commun.* **2009**, *74*, 167−188.

(8) For recent reviews of ion-mobility measurements of gaseous ions, see: (a) Kanua, A. B.; Dwivedi, P.; Tam, M.; Matz, L.; Hill, H. H., Jr. *J. Mass Spectrom.* **2008**, *43*, 1−22. (b) Bohrer, B. C.; Mererbloom, S. I.; Koeniger, S. L.; Hilderbrand, A. E.; Clemmer, D. E. *Ann. Rev. Anal. Chem.* **2008**, *1*, 293−327. (c) Puton, J.; Nousiainen, M.; Sillanpaa, M. *Talanta* **2008**, *76*, 978−987.

(9) (a) Révész, Á.; Schröder, D.; Rokob, T. A.; Havlík, M.; Dolenský, B. *Angew. Chem., Int. Ed.* **2011**, *50*, 2401−2404. (b) Schröder, D. *Collect. Czech. Chem. Commun.* **2011**, *76*, 351−369.

(10) See also: Pringle, S. D.; Giles, K.; Wildgoose, J. L.; Williams, J. P.; Slade, S. E.; Thalassinos, K.; Baterman, R. H.; Bowers, M. T.; Scrivens, J. H. *Int. J. Mass Spectrom.* **2007**, *261*, 1−12.

(11) (a) Schröder, D.; Weiske, T.; Schwarz, H. *Int. J. Mass Spectrom.* **2002**, *219*, 729−738. (b) Schröder, D.; Engeser, M.; Brönstrup, M.; Daniel, C.; Spandl, J.; Hartl, H. *Int. J. Mass Spectrom.* **2003**, *228*, 743−757. (c) Schröder, D.; Schwarz, H. *Can. J. Chem.* **2005**, *83*, 1936−1940. (d) Trage, C.; Diefenbach, M.; Schröder, D.; Schwarz, H. *Chem.—Eur. J.* **2006**, *12*, 2454−2464.

(12) To a much more limited but yet significant extent, also the temperature of the ion source influences the amount of fragmentation in the ionization region. For an example with correlations to the condensed phase, see: Agrawal, D.; Zins, E. L.; Schröder, D. *Chem. Asian J.* **2010**, *5*, 1667−1676.

(13) Vosko, S. H.; Wilk, L.; Nusair, M. *Can. J. Phys.* **1980**, *58*, 1200−1211.

(14) Lee, C.; Yang, W.; Parr, R. G. *Phys. Rev. B* **1988**, *37*, 785−789.

(15) Miehlich, B.; Savin, A.; Stoll, H.; Preuss, H. *Chem. Phys. Lett.* **1989**, *157*, 200−206.

(16) Becke, A. D. *J. Chem. Phys.* **1993**, *98*, 5648−5652.

(17) Frisch, M. J.; et al. *Gaussian 09*, Revision A.02; Gaussian, Inc.: Wallingford, CT, 2009.

(18) Tomasi, J.; Mennucci, B.; Cammi, R. *Chem. Rev.* **2005**, *105*, 2999−3093.

(19) For the first and second pK_a values of **1** in various cosolvent-water mixtures, see: Miklautz, H.; Keller, D.; Lopez Holguin, F.; Woloszczak, R *Anal. Bioanal. Chem.* **2006**, *384*, 1191−1195.

(20) For recent examples for a differentiation of various tautomers ("protomers") using IM-MS, see: Lalli, P. M.; Iglesias, B. A.; Toma, H. E.; de Sa, G. F.; Daroda, R. J.; Silva Filho, J. C.; Szulejko, J. E.; Araki, K.; Eberlin, M. N. *J. Mass Spectrom.* **2012**, *47*, 712−719.

(21) Cooks, R. G.; Wong, P. S. H. *Acc. Chem. Res.* **1998**, *31*, 379−386.

(22) In *Ion Mobility Spectrometry−Mass Spectrometry, Theory and Applications*; Wilkins, C. L., Trimpin, S., Eds.; CRC Press: New York, 2011.

(23) Bowers, M. T.; Kemper, P. R.; von Helden, G.; van Koppen, P. A. M. *Science* **1993**, *260*, 1446−1451.

(24) For dipole moment of ions, origin of coordinate system is at the center of mass, see: Serr, A.; Netz, R. R. *Int. J. Quantum Chem.* **2006**, *106*, 2960−2974.

(25) In addition, the concentration series shows a large increase of the relative abundance of the proton-bound dimer (m/z 275) with increasing concentration, as expected from the mass-action law. Thus, the relative fraction of the dimer rises from less than 1‰ at 10^{-6} M to about 10% at 10^{-2} M.

(26) Upon careful inspection of Figure 4, one may remark that the IM-MS resolution is somewhat worse for 10^{-2} M, which we observe more often when the total ion currents become large (presumably due to Coulomb broadening).

(27) For a possibility to convert the voltage scale into absolute collision energies, see: (a) Révész, Á.; Milko, P.; Žabka, J.; Schröder, D.; Roithová, J. *J. Mass Spectrom.* **2010**, *45*, 1246−1252. (b) Zins, E. L.; Pepe, C.; Schröder, D. *J. Mass Spectrom.* **2010**, *45*, 1253−1260. (c) Severa, L.; Jirásek, M.; Švec, P.; Teplý, F.; Révész, Á.; Schröder, D.; Kašička, V.; Koval, D.; Císařová, I.; Šaman, D. *ChemPlusChem* **2012**, *77*, 624−635.

(28) Here, integrated abundance is the sum of intensities of the parent ion with m/z 137 and the fragment at m/z 93 for the early and late components in the arrival-time distribution, i.e., $I(\mathbf{P}^-) = I(m/z\ 137)_{early} + I(m/z\ 93)_{early}$ and $I(\mathbf{C}^-) = I(m/z\ 137)_{late} + I(m/z\ 93)_{late}$, respectively. The fraction of $\mathbf{C}^-$ shown as the green trace in Figure 6 is accordingly obtained after normalization of $I(\mathbf{P}^-) + I(\mathbf{C}^-) = 1$.

(29) Solutions of **1** in D_2O should be measured immediately because within 0.5 h at ambient conditions a significant amount of deuterium into the ring protons is observed.

(30) Gunion, R. F.; Gilles, M. K.; Polak, M. L.; Lineberger, W. C. *Int. J. Mass Spectrom. Ion Processes* **1992**, *117*, 601−620.

(31) For theoretical studies of hydrogen bonding of **1** in the gas phase and in aqueous solution, see: Nagy, P. I.; Dunn, W. J.; Alagona, G.; Ghio, C. *J. Phys. Chem.* **1993**, *97*, 4628−4642.

(32) For spectroscopic studies of acetic acid in acetonitrile and other aprotic polar solvents, see: (a) Nakabayashi, T.; Nishi, N. *J. Phys. Chem. A* **2002**, *106*, 3491−3500. See also: (b) Reimers, J. R.; Hall, L. E. *J. Am. Chem. Soc.* **1999**, *121*, 3730−3744.
(33) (a) Tsierkezos, N. G.; Roithová, J.; Schröder, D.; Ončák, M.; Slavíček, P. *Inorg. Chem.* **2009**, *48*, 6287−6296. (b) Agrawal, D.; Schröder, D.; Sale, D. A.; Lloyd-Jones, G. C. *Organometallics* **2010**, *29*, 3979−3986. (c) Révész, Á.; Schröder, D.; Svec, J.; Wimmerová, M.; Šindelář, V. *J. Phys. Chem. A* **2011**, *115*, 11378−11386.
(34) (a) Cheng, J.; Vecitis, C. D.; Hoffmann, M. R.; Colussi, A. J. *J. Phys. Chem. B* **2006**, *110*, 25598−25602. (b) Cheng, J.; Hoffmann, M. R.; Colussi, A. J. *J. Phys. Chem. B* **2008**, *112*, 7157−7161. (c) Enami, S.; Hoffmann, M. R.; Colussi, A. J. *J. Phys. Chem. Lett.* **2010**, *1*, 1599−1604.
(35) For a comprehensive study of carboxylates at hydrophobic/water interfaces, see: Beaman, D. K.; Robertson, E. J.; Richmond, G. L. *J. Phys. Chem. C* **2011**, *115*, 12508−12516.
(36) In aggregates of free **1**, the aromatic system has been suggested to be oriented planar to the air/water interface, see: Weissbuch, I.; Berkovic, G.; Yam, R.; Als-Nielsen, J.; Kjaer, K.; Lahav, M.; Leiserowitz, L. *J. Phys. Chem.* **1995**, *99*, 6036−6045.
(37) For problems in the quantification of isomeric mixtures using IRMPD, see: Prell, J. S.; Chang, T. M.; Biles, J. A.; Berden, G.; Oomens, J.; Williams, E. R. *J. Phys. Chem. A* **2011**, *115*, 2745−2751.